X-621-69-255

SEASONAL VARIATIONS IN THE F_2 REGION

H.G. MAYR
K. MAHAJAN

JUNE 1969

GSFC
GODDARD SPACE FLIGHT CENTER
GREENBELT, MARYLAND

X-621-69-255

SEASONAL VARIATIONS IN THE F_2 REGION

H. G. Mayr
K. Mahajan

June 1969

Goddard Space Flight Center
Greenbelt, Maryland

SEASONAL VARIATIONS IN THE F_2 REGION

H. G. Mayr

K. Mahajan

ABSTRACT

Semiannual and annual variations in the F_2-region are discussed based on foF_2 and radar backscatter observations during the descending phase of solar activity (1958-1965). The semiannual effect appears as a persistent feature of the ionosphere which, demonstrably, is not related to fluctuations in the 10.7 cm noise or the EUV radiation. This gives support to theories that attribute the semiannual effec to variations in the lower atmosphere. Although theoretically predicted temperature variations (Volland, 1969) could quantitatively account for the observed semiannual variations in the height of the F_2-peak, the variations in N_mF_2 require additionally significant variations in the neutral composition at lower heights. Evidence for this is found in rocketborne $[O]/[O_2]$ measurements at 120 km which show maxima during equinox and a maximum to minimum ratio of two consistent with the ionospheric behavior. The annual variation in the ionosphere, showing a winter to summer enhancement in the F_2 peak density at low latitudes and during low solar activity, can be explained by meridional winds at ionospheric heights. These winds also have a significant effect on the height of the F_2 peak and appear to be effective throughout the solar cycle as

evident from radar backscatter observations, which show the peak at higher altitudes in summer than in winter. This is consistent with the observations of King et al., 1968, pointing out that the electron density in the topside ionosphere is persistently higher in the summer hemisphere than in the winter hemisphere thus suggesting that in the upper ionosphere the wind effect on the height of the F_2 maximum has masked the processes responsible for the winter anomaly in N_m.

SEASONAL VARIATIONS IN THE F_2 REGION

INTRODUCTION

There are two major anomalies in the seasonal behaviour of the daytime F-region. The first and the more widely discussed one is the winter anomaly where the winter F-region critical frequencies (foF2) are found to exceed those in summer, in particular at the higher latitudes and during the high solar activity (see e.g. Ratcliffe and Weekes, 1960 and references therein). The second, but not as widely discussed, is the semi-annual effect in foF2, with maxima in March and October and minima in July and January (see e. g. Burkard, 1951, Bhargava, 1959, Yonezawa and Arima 1959, Yonezawa, 1959). The winter anomaly has, in fact, been demonstrated to be really an electron density depression in summer, (see e. g. Wright, 1963) and has been proposed by Johnson (1964) and King (1964) to be due to molecular oxygen abundance in the summer hemisphere, arising from the global upper atmosphere circulation with air rising over the summer and settling over the winter hemisphere (Kellogg, 1961). While this argument has been re-supported by Duncan (1969) for the winter anomaly in his recent work, no attempts seem to have been made in the past to explain the semiannual effect. In this paper we shall re-study the seasonal variations in the daytime F-region and try to explain the semi-annual effect in foF2. We shall discuss the overall behaviour of the F-region in view of three kinds of mechanisms, namely: (i) neutral-ion drag effects due to horizontal meridional winds (King and Kohl, 1965),

(ii) changes in the neutral temperature (Volland 1969) and (iii) changes in the neutral composition, for which we shall present some experimental evidence.

DISCUSSION

The data employed in our investigation were bottomside sounder measurements of the critical frequency (foF_2) and radar backscatter observations of the height of the F_2 maximum (h_m) at Arecibo. In particular, the monthly means of these two parameters are considered, thus eliminating short term variations. We chose the data from 1600 local time which appear to be closest to the day-time maximum during the yearly variations. This choice was made to justify our steady state approach in solving the ion continuity equation for the F_2 region. However, this point is not critical because we have not attempted to reproduce actual values for height and density of the F_2 maximum but rather to match the yearly variations of these two parameters; and on this long time scale the assumption of steady state is certainly appropriate for the ionosphere.

Semiannual effects are observed both in the neutral and ionized components of the atmosphere. Burkard (1951) discovered first the semiannual effect in the F_2 -region. Patzold and Zschorner (1960) detected it in the thermospheric density, and subsequently semiannual variations were observed in the geomagnetic S_q variation (Wagner, 1968) in the geomagnetic activity (Priester and Cattani, 1962) in the height of the F_2 maximum (Becker, 1966), in the electric

and neutral components of the mesosphere (Lauter et al., 1966) and in the wind circulation within the mesosphere (Kochanski, 1963) and the stratosphere (Quiroz and Miller, 1967).

Several solar-terrestrial interaction mechanisms have been invoked to explain these effects: Pätzold and Tschörner (1960) and Priester and Cattani (1962) attribute the semiannual variation to the solar wind impinging on the magnetosphere. Chandra and Krishnamurthy (1968) pointed out that a correlation exists between the 10.7 cm solar radio noise and thus EUV radiation, and the semiannual variation in the gas temperature. Others invoke processes that occur in the lower atmosphere: Newell (1968) attributes it to a change in the mesospheric circulation system and Volland (1969) shows that the semiannual variations in the thermospheric temperature can be explained as resulting from tidal waves that are triggered by the mesospheric wind system. It will be shown here that ionospheric observations are consistent with the latter group of theoretical models.

Figure 1 reveals that a semiannual effect in N_m was present throughout the entire descending phase of solar activity. It is most pronounced at low latitudes with a ratio between maximum to minimum density of the order of 1.6. The variation is barely recognizable at midlatitudes.

As an indicator of the solar extreme ultraviolet, the 10.7 cm flux is shown for comparison. Its fluctuations reveal a maximum to minimum ratio of less

than 1.2. To the extent that the 10.7 cm flux represents the variations in the EUV radiation, its variations should correspond to fluctuations in both the thermospheric gas temperature and the electron production rate. An increase in the temperature enhances N_2 and O_2 more than O, thus tends to reduce the F_2 maximum density. However, the increase in the photoionizing EUV flux increases the electron density proportionally. Thus the electron density variations induced by fluctuations in the EUV (10.7 cm flux) are opposed by the increase in T_∞ which accompanies the flux-increase, and one therefore expects a smaller variation of $N_m F_2$ than 1.2. This value is significantly smaller than the observed ratio in the semiannual effect and we consider this as one evidence that the semiannual effect cannot be attributed primarily to the solar EUV radiation. It is, however, clear that EUV fluctuations are not negligible when superimposed on the semiannual variations and this may be responsible for the positive correlation that sometimes exists between the 10.7 cm flux and the electron density in periods when this flux shows a quasi-half year period. Additional evidence that the fluctuations in the 10.7 cm flux are not responsible for the semiannual effect (as a prevailing phenomenon) can be derived from the fact that summing the mean monthly 10.7 cm values over a solar cycle (1958-1969) does not reveal a significant semiannual effect. A similar conclusion was arrived at by Newell (1968).

Volland's (1969) theory of the semiannual effect in the thermosphere is based on a wave energy input from the lower atmosphere that produces an almost constant temperature increase at all altitudes in the thermosphere. Figure 2

shows N_m and h_m calculated (see Appendix) for a 100° temperature enhancement for minimum and maximum solar activity conditions. Furthermore, we show these parameters as functions of the composition ratio $[O]/[O_2]$ at 120 km. Assuming this to reflect only variations in O we adopted a similar variation in the $[O]/[N_2]$ ratio.

From Figure 2 it is apparent that a temperature increase of 100°K can only produce an electron density maximum to minimum ratio of 1.15, small compared with the observed value of 1.6. The temperature effect on h_m is significant however as it increases h_m by 35 km during minimum solar activity and by 45 km during maximum solar activity. This appears to be consistent with observations by Becker (1966) which show semiannual variations in h_m of this order.

As the $[O]/[O_2]$ and $[O]/[N_2]$ ratios significantly affect the F-region electron densities, we have collected all the neutral composition measurements to date (see Table 1) to look for any semiannual effect in these quantities. Figure 3 shows a definite indication of a semiannual effect in the $[O]/[O_2]$ ratio at 120 km, although some of this variability may be attributed to the somewhat different measurement techniques employed in these rocket experiments. Furthermore, neutral composition measurements (References from Table 1) show significant variability in the $[O]/[N_2]$ ratio (not shown here) while simultaneously $[N_2]$ remains constant. Unfortunately, the few data available on the latter ratio are insufficient to provide information on its semiannual

component. Variations in the neutral composition as described in Figure 3 are more than sufficient to produce the semiannual variations in the F_2 -maximum density as demonstrated in Figure 2). The observed variations in the electron density are in fact less than the composition amplitude would require.

Annual Variations

During low solar activity and at low latitudes N_m is larger in summer than in winter (Figure 1). Furthermore, radio backscatter observations of h_m in Puerto Rico (Figure 4) show that this parameter increases by about 100 km from winter to summer.

Composition changes as shown in Figure 3 cannot account for these effects because they are not in phase with the summer enhancement and, moreover, they do not affect h_m appreciably. Furthermore, reasonable variations in the gas temperature would also not produce enough variation of both electron density and h_m.

King and Kohl (1965) and many other investigators have stressed that horizontal meridional winds in the neutral atmosphere significantly affect the distribution of the ionospheric plasma. Kohl and King (1967), Geisler (1966) and Volland and Mayr (1969) deduced the wind field from the empirical atmospheric model that Jacchia (1964) derived from satellite drag measurements. A gross feature of this wind field is that the winds blow away from the atmospheric pressure bulge that forms at the subsolar point (Jacchia and Slowey, 1966) and that

the wind velocities increase away from the subsolar point toward the poles. During the year the subsolar latitude moves between 23.5 north and south geographic. At American longitudes (where the ionosphere data were taken) the subsolar point is at 37°N geomagnetic latitude at summer solstice and at 11°S at winter solstice. Thus at low latitudes in summer the daytime winds blow toward the equator. As only the wind component parallel to the magnetic field affects the ionosphere, these equatorward winds produce at low latitudes an upward drift of ionization that enhances height and density of the F_2 peak. Conversely, during winter the winds blow away from the equator and produce corresponding downward ionization drifts that decrease both height and density of the F_2-maximum. Thus winds can reasonably be invoked to produce winter to summer enhancements in the ionization and peak height of the F_2-region.

The approach of Volland and Mayr (1969) is here adopted to describe the structure of the meridional thermosphere winds by means of spherical functions of low degree:

$$u = u_{10} P_{10} \cos \lambda + u_{21} \frac{P_{21}}{\cos \lambda} \cos (\omega(\tau - \tau_{21})) \qquad (1)$$

where

$$P_{10} = \sin \lambda$$

$$P_{21} = \frac{3}{2} \sin (2\lambda)$$

λ = geographic latitude

$\tau = \tau + \frac{\ell}{\omega}$ (local time)

τ = universal time

$\omega = \frac{2\pi}{\tau_0}$ (angular frequency with τ_0 the period of one day)

ℓ = geographic longitude

τ_{21} = 1400 local time (observed diurnal maximum in atmospheric density)

u is positive in fourth direction.

Equation (1) is only valid for equinox conditions but with an appropriate transformation it can be formally adapted to describe also winter or summer conditions. In this paper we shall not go into the details of this modification, but rather restrict ourselves to the very simple case where the diurnal density maximum occurs at noon geomagnetic local time (at American longitudes). Then we are justified to replace λ by $(\lambda - \eta)$, where η is the inclination of the sun to the geographic equator ($\eta = 23.5°$ for summer and $\eta = -23.5°$ for winter). At American longitudes the magnetic equator is south of the geographic equator and thus we can describe the wind field by substituting in equation (1) $\lambda = (\theta + 13°)$ where we define θ on the geomagnetic latitude. With I the magnetic dip angle, the wind component parallel to the magnetic field is $u_{\parallel} = u \cos I$. The vertical wind component, that enters into the ion continuity equation is then

$$u_{\perp} = u_{\parallel} \sin I = u \cos I \sin I;$$

Its latitudinal distribution is shown in Figure 5, for summer, winter and equinox conditions in the northern hemisphere.

For illustrative purpose, we show in Figure 6 several electron density profiles which were computed for minimum solar activity conditions (at 30° geomagnetic latitude) employing upward and downward wind components. From this diagram it is evident that the winds, shown in Figure 5, can quantitatively account for the observed variations in h_{max} (Figure 4) and N_{max} (Figure 1) during low solar activity. A feature of the electron density distribution in Figure 6 is that upward winds are much more effective in increasing N_m and h_m than downward winds are in decreasing these parameters. (This is to be expected since downward winds bring the F_2-layer closer to the chemical equilibrium region.) For this reason it is understandable that the wind effects are most pronounced in N_m at low latitudes where, according to Figure 5 the upward wind components are largest.

Our interpretation of the summer enhancement of N_m by atmospheric winds appears only satisfactory for minimum solar activity conditions. Figure 1 reveals that during high solar activity the semiannual effect prevails at low latitudes while the winter anomaly, with higher density values in winter than in summer, prevails at midlatitudes.

It was pointed out by Geisler (1966) and Volland (1969) that the magnitude of the winds are controlled primarily by ion-neutral drag rather than viscosity

affects. Thus, at high solar activity the greater electron density tends to increase the ion drag and to decrease the wind velocity. But at high solar activity the pressure in the neutral atmosphere is also enhanced and this would tend to increase the wind effect in F_2 region heights. The observations of the height of F_2 maximum (Figure 4) show that the ratio of the winter to summer enhancement did not change significantly between 1958 and 1965, which suggests that wind effects are of comparable importance throughout the solar cycle. Therefore, other mechanisms must be invoked at high solar activity to selectively depress and mask the summer enhancement of N_m (but not h_m) that is so apparent during low solar activity.

As shown earlier, variations in the neutral composition can affect N_m without considerably changing h_m. Thus, we infer that during high solar activity $[O]/[O_2]$ and $[O]/[N_2]$ decrease from winter to summer* and thus decrease N_m in summer relative to its value in winter. This effect could counter balance or even neutralize the summer enhancement that would normally be produced by wind effects. Therefore it is understandable that at low latitudes the semiannual effect prevails. At midlatitudes the wind effects are smaller and therefore the composition changes prevail with the result that the winter values of N_m are enhanced over those in summer.

*Most of the measurements in Table 1 and Fig. 3 correspond to periods of low solar activity and thus we cannot check on this postulation.

The atmospheric composition changes required to produce the winter anomaly, are predicted in the circulation theory by Kellogg (1961), Johnson (1964a) and King (1964). These authors propose that solar heating in the lower ionosphere induces upwelling of atmospheric molecular species over the summer, and settling of atomic oxygen over the winter hemisphere. As the ionospheric heating increases with increasing solar activity, it is understandable that this mechanism would be primarily effective during maximum solar activity which is consistent with the existence of the winter anomaly.

King et al. (1968) reported that topside sounder observations do not show the winter anomaly. This behavior supports further the wind effects discussed before if we consider that the electron density in the topside ionosphere not only depends on N_m but very significantly also on h_m (see Figure 6). The latter of both reveals the wind effect throughout the entire period of changing solar activity (see Figure 4), thus tends to produce winter to summer enhancements in the electron density of the topside ionosphere.

SUMMARY AND CONCLUSION

We have discussed foF_2 observations over a wide range of latitudes and throughout the descending phase of solar activity (1958-1965), and radio backscatter observations of the height of the F_2 maximum and Arecibo between 1958 and 1965.

The semiannual variation in N_m appears as a persistent feature of the ionosphere. Fluctuations of solar EUV indicated by the 10.7 cm radio noise are found to be quantitatively insufficient to account for the observed amplitude of the semiannual N_m variation, furthermore we do not see a prevailing semiannual component in the 10.7 cm flux over a solar cycle. For these reasons solar EUV must be excluded as the primary source for the semiannual effect.

The ionospheric evidence supports theories that attribute the semiannual effect to variations in the lower atmosphere (Newell, 1968, Volland, 1969). To explain the ionospheric density variations, semiannual variations in the neutral composition are required. We find some evidence from the few available neutral composition measurements that the ratio $[O]/[O_2]$ varies by a factor of two and is greatest during equinox. The phase and amplitude is consistent with the semiannual variation in N_m.

In a subsequent paper, an attempt is made to explain this composition effect by invoking the global wind circulation within the lower atmosphere (Mayr, Newton, Volland, and Mahajan, 1969).

The annual component in the ionosphere showing a winter to summer enhancement in N_m at low latitudes and low solar activity, can be explained as resulting from horizontal atmospheric winds. Observations of the height of the F_2 maximum at Arecibo show a strong annual variation at all levels of solar activity.

These annual changes in h_m constitute important additional evidence for atmospheric winds, thus indicating that winds are effective throughout the solar cycle.

The latter we suggest as an explanation for the fact that the winter anomaly is not observed in the topside ionosphere (King, et al., 1968).

ACKNOWLEDGMENT

We are very indebted to L. H. Brace and H. A. Taylor, Jr. for many valuable suggestions.

REFERENCES

1. Becker, W., Electron Density Profiles in Ionosphere and Exosphere, North-Holland Publ. Comp., Amsterdam, Space Res., 5, 1966

2. Bhargava, B. N. "Annual Wave in the World Wide F-region Ionization," Indian J. Meteorol. Geophys. 10, 69, 1959

3. Brace, L. H., N. W. Spencer and A. Dalgarno, Detailed Behavior of the Mid-latitude Ionosphere from Explorer XVII Satellite, Planet. Space Sci., 13, 647-666, 1965

4. Burkard, O., "Die halbjahrige Periode der F2 – Schichtionisation," Arch. Meteorol. Geophys. Bioklimatol, A4, 391, 1951

5. Chandra, S. and B. V. Krishnamurthy, The Response of the Upper Atmospheric Temperature to Changes in Solar EUV Radiation and Geomagnetic Activity, Planet. Space Sci., 16, 231-242, 1968

6. Colegrove, F. D., W. B. Hanson and F. J. Johnson, Eddy Diffusion and Oxygen Transport in the Lower Thermosphere, J. Geophys. Res., 70, 4931-4941, 1965

7. Doupnik and Nisbet, Fluctuations of the Electron Density in the Daytime F-Region, J. Atmosph. Terrest. Phys., 30, 931-961, 1968

8. Garriott, O. K., F. L. Smith, and P. C. Yuen, Observation of Ionospheric Electron Content Using a Geostationary Satellite, Planet. Space Sci., 13, 1829, 1965

9. Gross, J., D. Offermann, and U. von Zahn, Neutral Particle Densities in the Lower Thermosphere as Measured by Mass Spectrometers Above Fort Churchill and Sardinia, Space Res., 8, 920-925, 1968

10. Hedin, A. E., and A. O. Nier, A Determination of the Neutral Composition, Number Density, and Temperature of the Upper Atmosphere from 120 to 200 Kilometers with Rocket Borne Mass Spectrometers, J. Geophys. Res., 71, 4121-4131, 1966

11. Jacchia, L. G., Static Diffusion Models of the Upper Atmosphere with Empirical Temperature Profiles, Research in Space Science, 70, 1964

12. Jacchia, L. G. and J. Slowey, The Shape and Location of the Diurnal Bulge in the Upper Atmosphere, Research in Science, Report 207, 1966

13. Jones, K. L., Distribution of Atmospheric Ionization in the Region 15° to 30° South Latitude, Planetary Space Sci., 16, 385, 1968

14. Johnson, F. S., Composition Changes in the Upper Atmosphere in "Electron Density Distribution in Ionosphere and Exosphere," Proceedings of NATO Advanced Institute, Sheikempen, Norway, 1963

15. Kasprzak, W. T., D. Krankowsky, and A. O. Nier, A Study of Day-Night Variations in the Neutral Composition of the Lower Thermosphere, J. Geophys., Res., 73, 6765-6782, 1968

16. Kellogg, W. W., Chemical Heating Above the Polar Mesosphere in Winter, J. Meteorology, 18, 373-381, 1961

17. King, G. A. M., The Dissociation of Oxygen and High Level Circulation in the Atmosphere, J. Atmosph. Sci., 21, 231-237, 1964

18. King, J. W., G. L. Hawkins, and C. Seobrook, The Seasonal Behavior of the Topside Ionosphere, J. Atmosph. Terr. Phys., 30, 1701-1706, 1968

19. Klobuchen, J. A. and H. E. Whitney, Middle Latitude Ionospheric Electron Content: Summer 1965, Radio Sci., 1, 1149, 1966

20. Kochanski, A., Circulation and Temperatures at 70- to 100-Kilometer Height, J. Geophys. Res., 68, 213-226, 1963

21. Kohl, H., and J. W. King, Atmospheric Winds Between 100 and 700 km and Their Effects on the Ionosphere, J. Atmosph. Terrest. Phys., 29, 1045, 1967

22. Krankowsky, D., W. T. Kasprzak, and A. O. Nier, Mass Spectrometer Studies of the Composition of the Lower Thermosphere During Summer 1967, J. Geophys. Res., 73, 7291-7306, 1968

23. Lauter, E. A., J. Hruskova, G. Nestroiov, and K. Sprenger, Vorträge Sommerschule Kuhlungsborn, Vol. II/1, Berlin, 1966

24. Mahajan, K. K., Extent of Thermal Nonequilibrium in the Ionosphere, J. Atmosph. Terrest. Phys., 29, 1137, 1967

25. Mahajan, K. K., P. B. Rao, and S. S. Prasad, Incoherent Backscatter Study of Electron Content and Equivalent Slab Thickness, J. Geophys. Res., 73, 2477, 1968

26. Mauersberger, K., D. Müller, D. Offermann, and U. von Zahn, Neutral Constituents of the Upper Atmosphere in the Altitude Range of 110 to 160 km Above Sardinia, Space Res., 7, 1150-1158, 1967

27. Mayr, H. ..., G. P. Newton, H. E. Volland and K. K. Mahagan, Semiannual Variations in the Neutral Composition, NASA Document X-621-69-278.

28. Newell, R. E., Semiannual Variation in Thermospheric Density, Nature, 217, 150-151, 1968

29. Nier, A. O., J. H. Hoffman, C. Y. Johnson, and J. C. Holmes, Neutral Composition of the Atmosphere in the 100- to 200-Kilometer Range, J. Geophys. Res., 69, 979-989, 1964

30. Pätzold, H. K. and H. Zschörner, Bearings of Sputnik III and the Variable Acceleration of Satellites, Space Res., 1, 1960

31. Pokhunkov, A. A., On the Variation in the Mean Molecular Weight of Air in the Night Atmosphere at Altitudes of 100 to 210 km from Mass Spectrometer Measurements, Planetary Space Sci., 11, 297-304, 1963a

32. Pokhunkov, A. A., Gravitational Separation, Composition and Structural Parameters of the Night Atmosphere at Altitudes Between 100 and 210 km, Planetary Space Sci., 11, 441-449, 1963b

33. Pokhunkov, A. A., Gravitational Separation Composition, and the Structural Parameters of the Atmosphere at Altitudes Above 100 km, Space Res., 3, 132-142, 1963c

34. Priester, W. and D. Cattani, On the Semiannual Variation of Geomagnetic Activity and its Relation to the Solar Corpuscular Radiation, J. Atm. Sci., 19, 121-126, 1962

35. Quiroz, R. S. and A. J. Miller, Note on the Semiannual Wind Variation in the Equatorial Stratosphere, Monthly Weather Rev., 95, 635-641, 1967

36. Schaefer, E. J., and M. H. Nichols, Upper Air Neutral Composition Measurements by a Mass Spectrometer, J. Geophys. Res., 69, 4649-4660, 1964

37. Schaefer, E. J., Neutral Composition, Sci. Rept. 05627-3-S, High Altitude Eng. Lab., The University of Michigan, 1966

38. Schaefer, E. J., Temperature and Composition of the Lower Thermosphere Obtained from Mass Spectrometer Measurements, Space Res., 8, 959-968, 1967

39. Titleridge, J. E., Continuous Records of the Total Electron Content of the Ionosphere, J. Atmosph. Terrest. Phys., 28, 1135, 1966

40. Volland, H., and H. Mayr, On the Diurnal Tide Within the Thermosphere, NASA-document X-621-68-444, 1968

41. Volland, H., A Theory of Thermospheric Dynamics, Part II: Geomagnetic Activity Effect, 27 Day Variation and Semiannual Variation, Planet. Space Sci., 1969

42. Wagner, C. U., About a Semiannual Variation of the Amplitude of the Geomagnetic Sq-Variations in Median Latitudes, J. Atmosph. Terr. Phys., 30, 579-589, 1968

43. Wright, J. W. "The F-region Seasonal Anomaly," J. Geophys. Res., 68, 4579, 1963

44. Yonezawa T., "On the Seasonal and Non Seasonal Annual Variations and the Semiannual Variation in the Noon and Midnight Electron Densities of the F2 Layer in Middle Latitudes" II, J. Rad. Res. Lab. (Japan) 6, 651, 1959

45. Yonezawa, T and Y. Arima, "On the Seasonal and Nonseasonal Annual Variations and the Semiannual Variation in the Noon and Midnight Electron Densities of the F2 Layer in Middle Latitudes," J. Rad. Res. Lab. (Japan) 6, 293

46. Yonezawa, T. and Y. Arima, On the Seasonal and Non-Seasonal Variations and the Semiannual Variation in the Noon and Midnight Electron Densities of the F 2 Layer in Middle Latitudes, J. Radio Res., 6, 293-309, 1959

APPENDIX

It is here assumed that O^+ is the major ion constituent within a neutral atmosphere where atomic oxygen, O, is the predominant neutral constituent. The oxygen ion density is then controlled by photoionization of O with a production rate Q, charge transfer to molecule N_2 and O_2 with a loss rate $L[O^+]$, and diffusion of O^+ through O with a transport velocity V_{O^+} parallel to the magnetic field. In steady state, the continuity equation has the form

$$Q - L[O^+] - B\frac{\partial}{\partial s}\left(\frac{[O^+]\ V_{O^+}}{B}\right) = 0 \qquad (1)$$

where

s is the distance along a field line and B is proportional to the intensity of the magnetic field,

$$B = \frac{1}{r^2}\ (1 + 3\cos^2\theta)^{1/2} \qquad (2)$$

therefore accounting for the divergence of the magnetic field tubes.

Conservation of momentum requires that the momentum equation

$$\theta_{O^+O}\ [O]\ [O^+]\ (V_{O^+} - V_{||}) = -\ kT\frac{\partial [O^+]}{\partial s} - mg_{||}\ [O^+] \qquad (3)$$

is satisfied, where

$\theta_{O^+O} = 2 \times 10^{-32}$ (cgs), drag coefficient for collisions between O^+ and O,

$V_{\parallel}$ = velocity component of O parallel to the magnetic field,

$T = (T_e + T_i)/2$

T_e = electron temperature, T_i = ion temperature

k = Boltzmann constant

m = mass of O^+

$g_{\parallel}$ = gravitational acceleration parallel to the magnetic field.

Jacchia's model (1965) was adopted for atomic oxygen, molecular nitrogen and oxygen, and gas temperature. The loss coefficient for charge transfer from O^+ to N_2 was chosen to be 2×10^{-12} cm^3 sec^{-1} and for O^+ to O_2 to be 1×10^{-11} cm^3 sec^{-1}. The photoionization probability was assumed to be $5 \times 10^{-7} \times \bar{F}/80$, where $\bar{F}$ is the 10.7 cm flux (10^{-22} w/m^2 c/s). Attenuation of the ionizing EUV radiation has been rigorously taken into account. For the electron temperature we used 1500°K which is consistent with satellite measurements by Brace et al. (1965). The ion temperature was assumed equal to the gas temperature an assumption that is justified from energetic considerations.

Integrating Equation (1) along a field line up to the equator yields

$$V_{O^+}[O^+] = \frac{B}{B_e} V_{O^+_e}[O^+] - B \int_s^{s_e} (Q - L[O^+]) \frac{ds}{B} \qquad (4)$$

where subscript e refers to the field line intersection in the equatorial plane. Combining Equations (3) and (4) one arrives at the differential-integral equation

$$kT \frac{\partial [O^+]}{\partial s} + mg_{\parallel} [O^+] = \alpha_{O^+O} [O] \left\{ [O^+] V_{\parallel} + B \int_s^{s_e} (Q - L[O^+]) \frac{ds}{B} - \frac{B}{B_e} V_{O^+} [O^+] \right\} \quad (5)$$

Representing the right hand side of Equation (5) by $D(s_1 [O^+])$ and assuming this function to be known, this equation can then be integrated thus yielding the integral equation

$$[O^+] = [O^+]_0 \exp \left\{ (s - s_0) \left[\frac{D(s_1 [O^+])}{[O^+]} - \frac{mg_{\parallel}}{kT} \right] \right\} \quad (6)$$

Equation (6) is solved for the following boundary conditions:

1. At low altitudes O^+ is assumed to approach the value determined by photochemical equilibrium

$$[O^+]_0 = \frac{Q}{L} .$$

2. In case of symmetry with respect to the equatorial plane (equinox condition) it is required that

$$V_{O^+ e} = 0 .$$

The solution of Equation (6) was accomplished by means of an iterative procedure in which the function $D(s_1 [O^+])/[O^+]$ was treated as a perturbation in the following scheme:

For the k th solution the perturbation function was assumed to be

$$\frac{D(s_1 [O^+]_k)}{[O^+]_k} = \epsilon_k \frac{D(s_1 [O^+]_{k-1})}{[O^+]_{k-1}}$$

where ϵ_k is a parameter that varied between

$$0 \leq \epsilon_{k-1} < \epsilon_k < \epsilon_{k+1} \leq 1$$

For the initial solution we assumed $\epsilon_1 = 0$ which is equivalent with diffusive equilibrium. In subsequent solutions ϵ_k is gradually increased to allow the perturbation function to become effective slowly. This procedure assures the applicability of the perturbation method which demands small effects from the "perturbing" function. A successive application of this procedure leads then to a convergence on the solution of Equation (6) when ϵ_k approaches 1.

One can immediately verify that this solution procedure requires the more iterations the larger the chemical terms are when compared to the transport terms in the continuity equation. This imposes a lower altitude limit for reasonably fast convergence. Employing an IBM 360-75 computer we started at 180 km and we achieved computer solutions accurate to better than 1% in 20 seconds of computing time.

Table 1

O and O_2 Number Density Ratios at 120 km Measured by Rocket-Borne Mass Spectrometers

$S_{10.7}$	Date	Time	Latitude	$n(O)/n(O_2)$	Reference
175	Sept. 23, 1960	0050 LT	'Middle'	0.72	Pokhunkov (1963a, b, c)
95	May 18, 1962	1302 EST	38°N	(1.2)	Schaefer and Nicholas (1964)
73	Mar. 28, 1963	0255 LT	38°N	1.2	Schaefer (1966)
77	June 6, 1963	0730 MST	33°N	0.78	Nier et. al. (1964)
82	Nov. 26, 1963	1316 LT	38°N	1.2	Schaefer (1967)
72	Feb. 18, 1965	1409 LT	59°N	0.75	Schaefer (1967)
72	Feb. 19, 1965	0317 LT	59°N	0.75	Schaefer (1967)
75	Apr. 15, 1965	0345 MST	33°N	0.33	Hedin and Nier (1966)
75	Nov. 30, 1966	0445 MST	33°N	(0.5)	Kasprzak et. al. (1968)
98	Dec. 2, 1966	1409 MST	33°N	0.46	Kasprzak et. al. (1968)
76	Dec. 11, 1965	0505 MET	40°N	1.56	Mauersberger et. al. (1967)
163	Dec. 12, 1966	1320 CST	59°N	0.87	Gross et. al. (1968)
119	June 21, 1967	1249 MST	33°N	0.55	Krankowsky et. al. (1968)
131	July 20, 1967	0200 MST	33°N	0.41	Krankowsky et. al. (1968)
131	July 20, 1967	1224 EST	33°N	0.41	Krankowsky et. al. (1968)

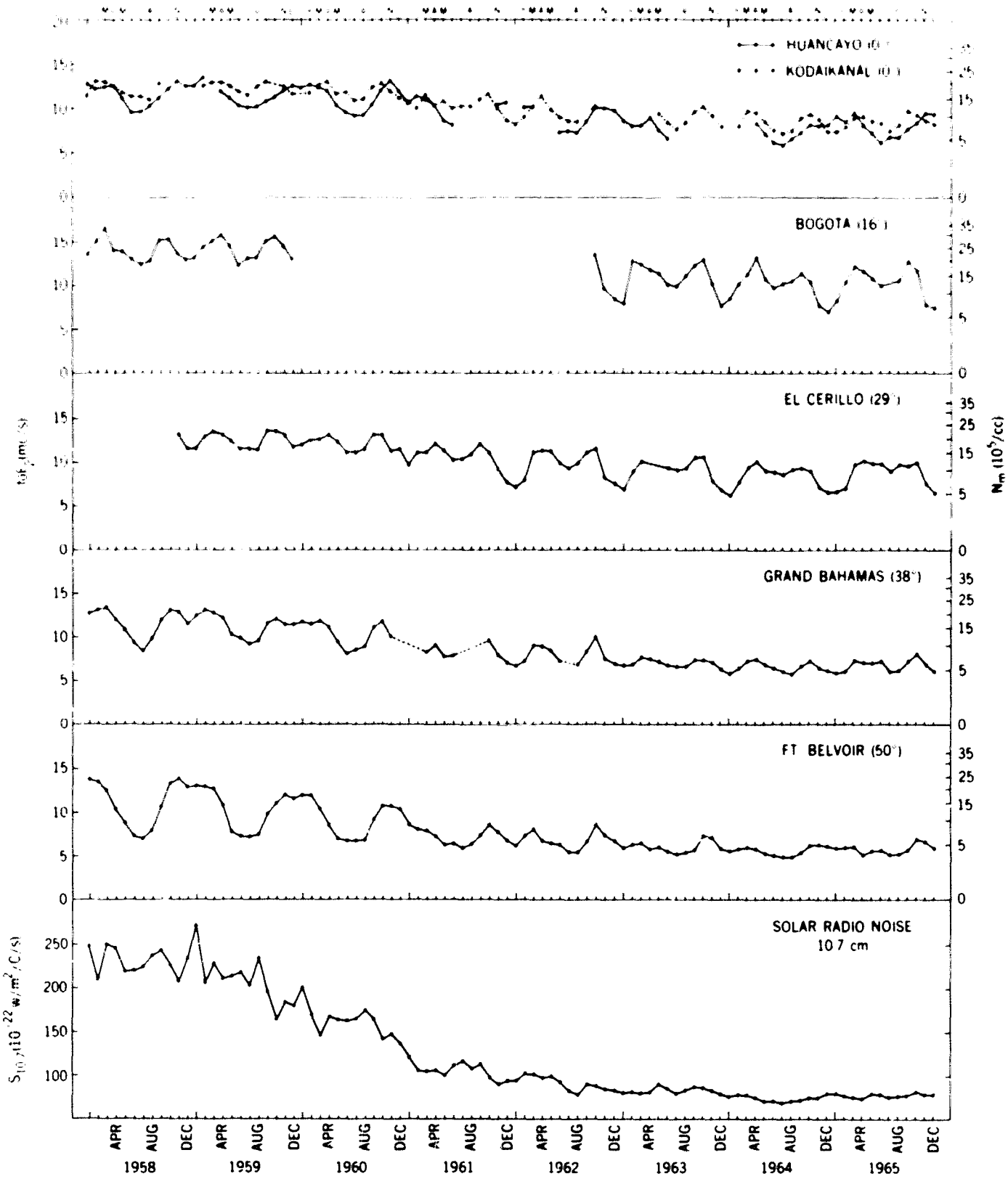

Figure 1. Monthly means of foF_2 and N_m for 1600 LT, and for comparison the 10.7 cm flux are shown during the descending phase of solar activity (1958–1965).

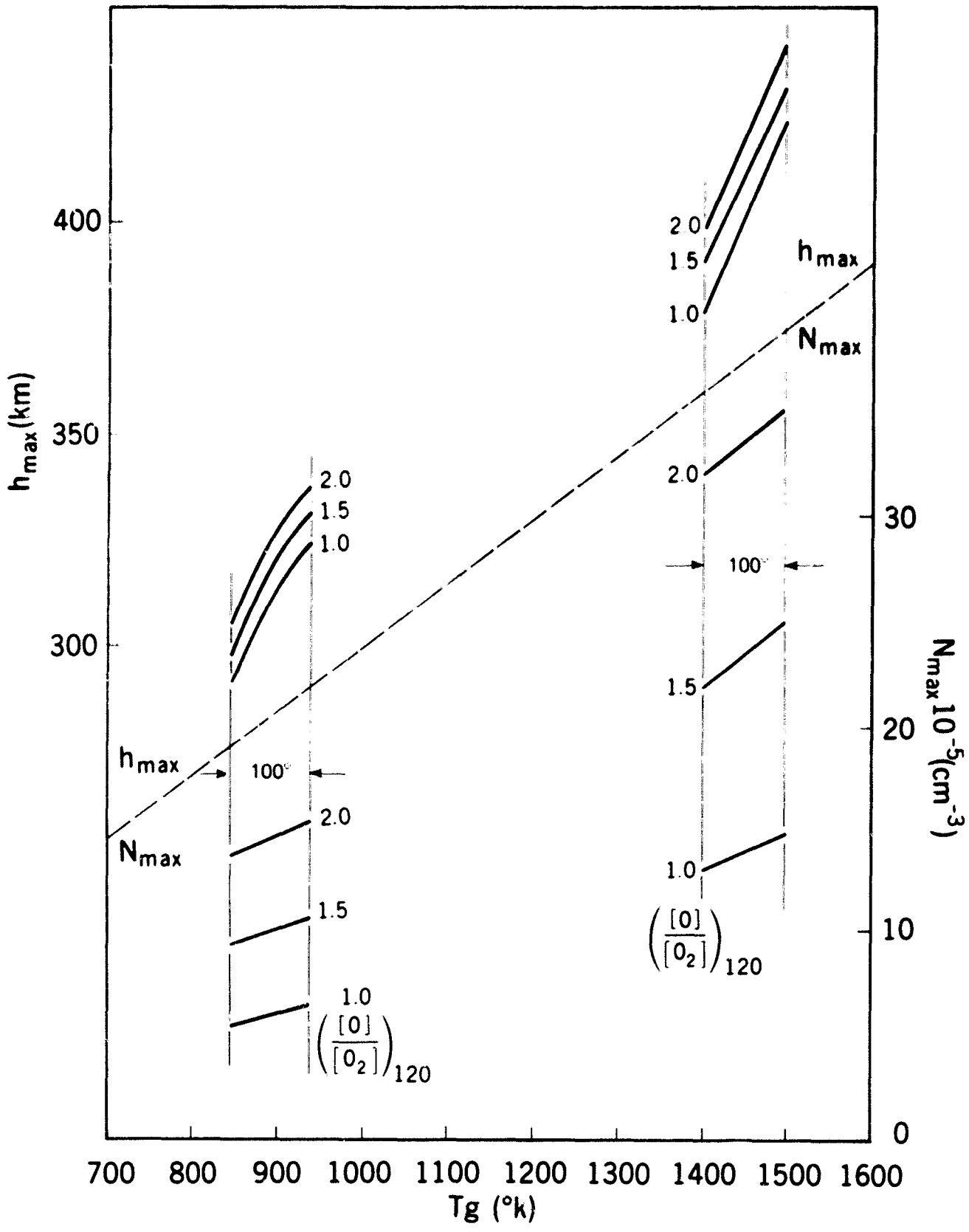

Figure 2. Computed N_{max} and h_{max} as functions of the $[O]/[O_2]$ ratio at 120 km varying from one to two, and furthermore depending on a constant temperature increase in the entire thermosphere (T_g is the exospheric gas temperature). Solid lines show the variability during minimum and maximum solar activity. The thin lines demonstrate the variations during the increasing phase of solar activity.

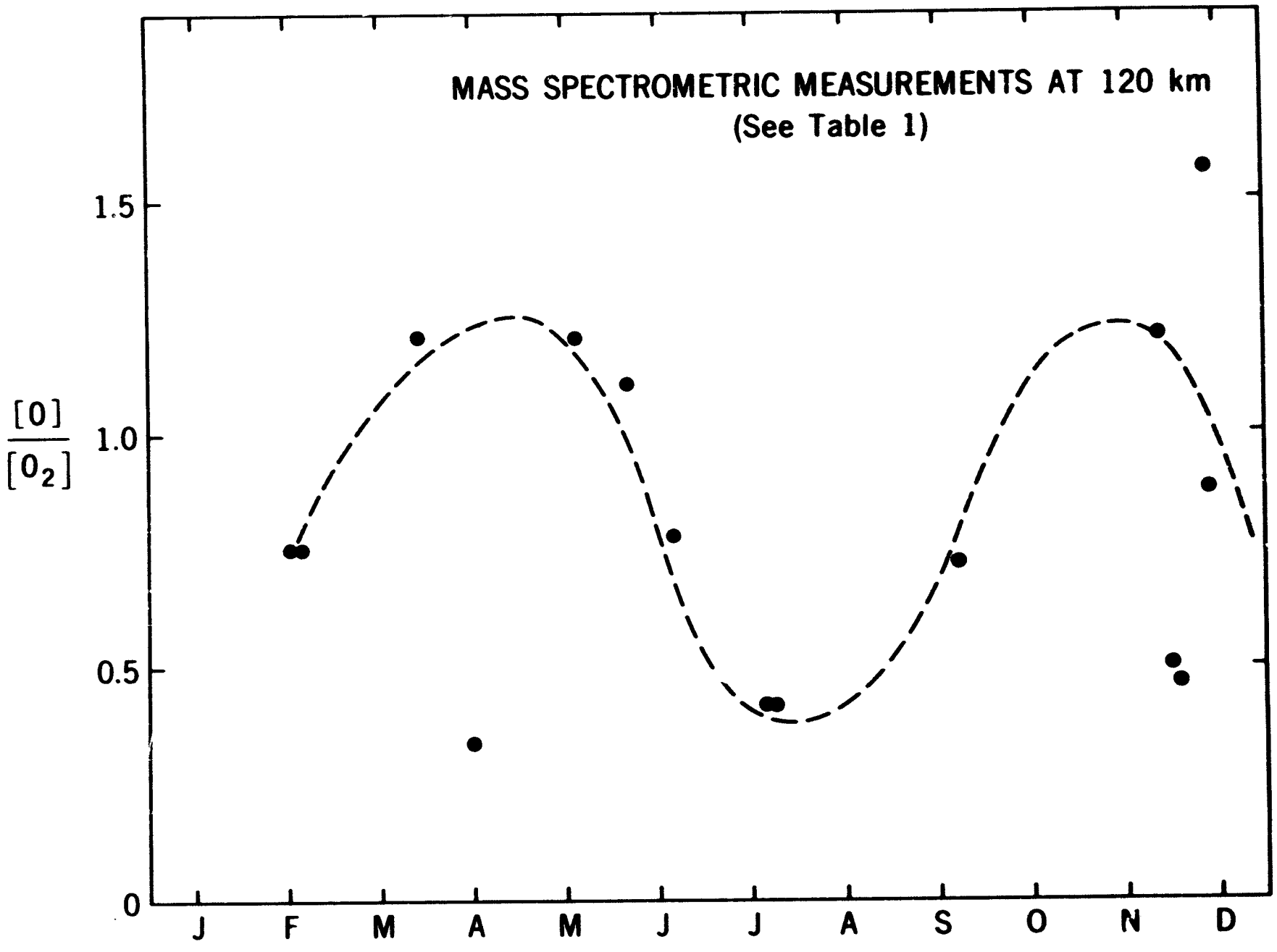

Figure 3– $[O]/[O_2]$ ratio at 120 km plotted from measurements referred to in Table 1. Note that the majority of data points exhibits a few annual variation (observed live).

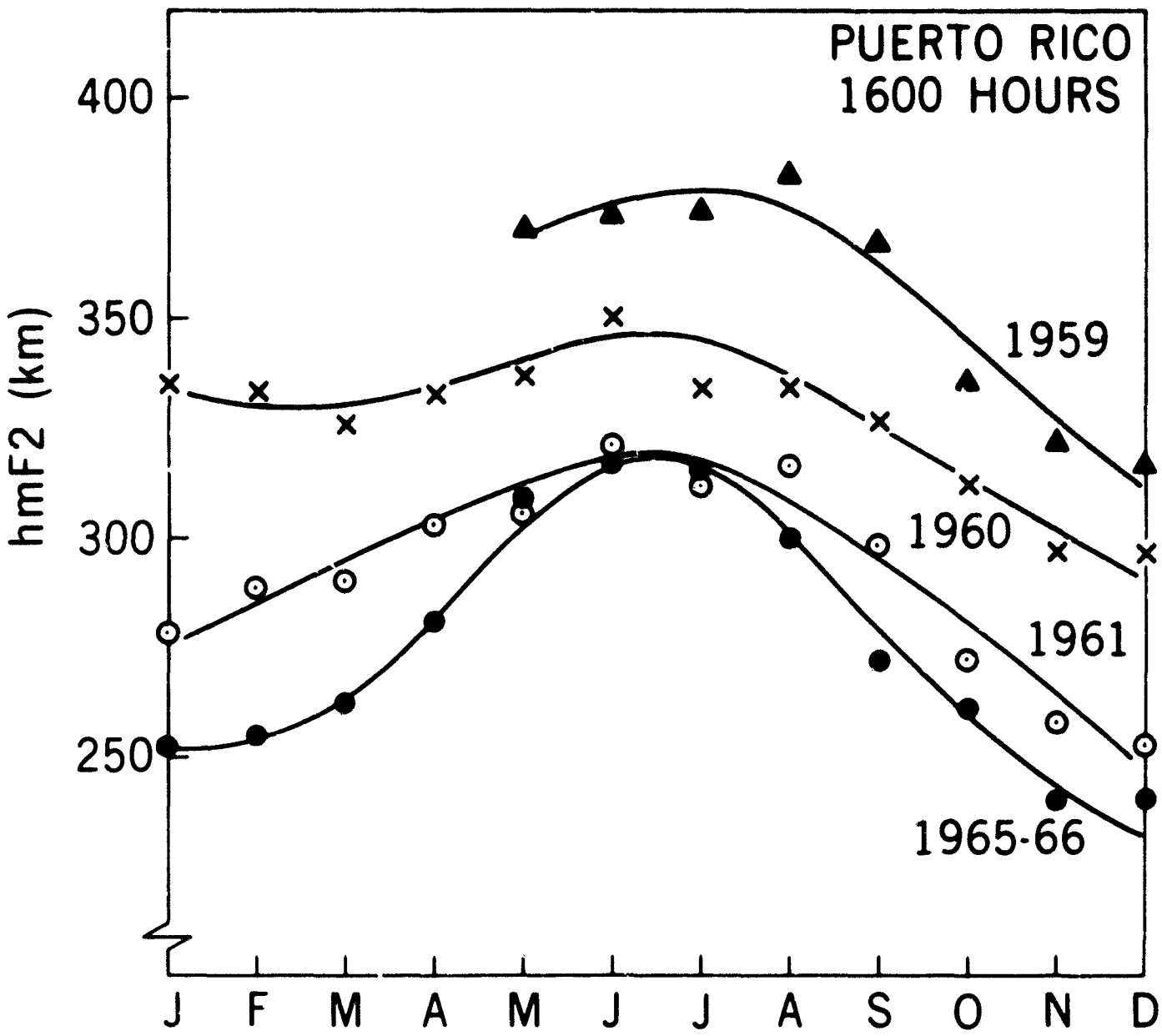

Figure 4. Monthly means of h_mF_2 during noon time derived from radar backscatter observations at Puerto Rico (1959 through 1966).

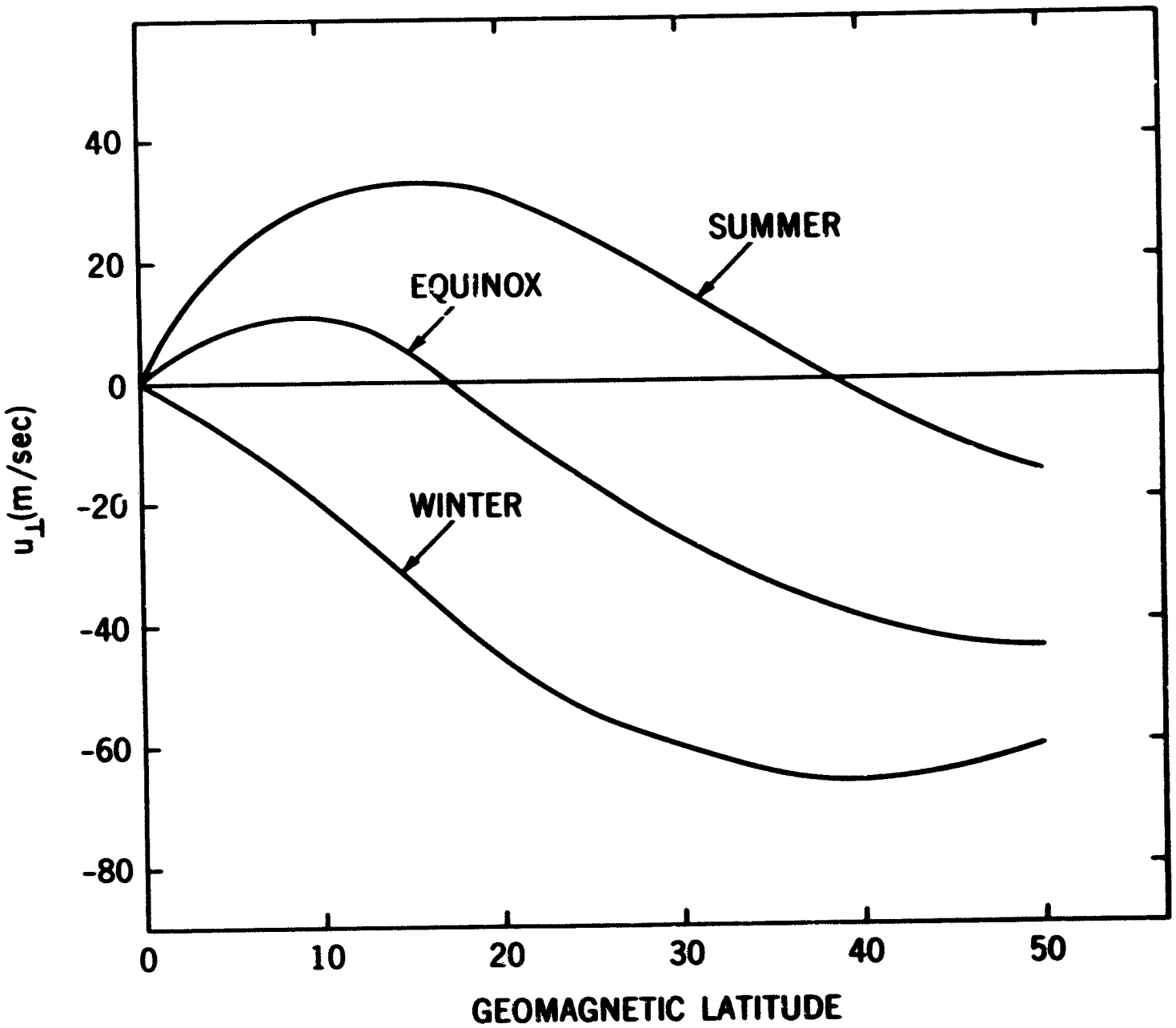

Figure 5. Vertical component of the meridional wind field shown for equinox, summer and winter in the northern hemisphere.

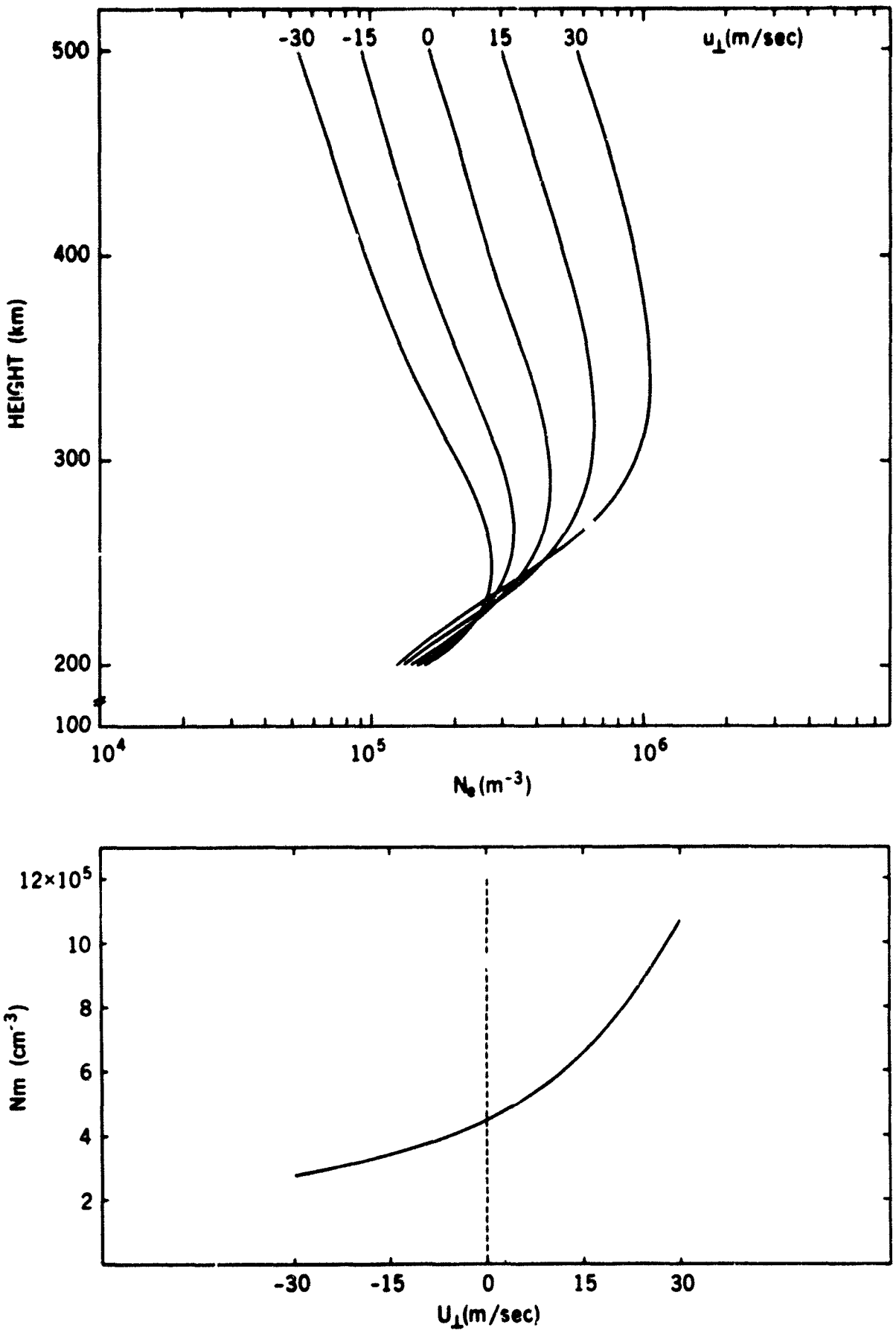

Figure 6. Computed electron density distributions for various wind magnitudes. Note at the bottom the non linear relation between wind velocity and the maximum electron density.